Ocean Ultrasonic Shear and Compression Viscosities

Josè V. Alemán[*,1], Pablo Sangrà[1] and Rafael Carbó[2]

[1]*Facultad de Ciencias del Mar, Campus Universitario de Tafira, 35017 Las Palmas de Gran Canaria, Spain*

[2]*Centro de Tecnologias Fisicas (CSIC),Serrano 144, 28006 Madrid, Spain*

Abstract: A comprehensive description of ocean molecular flow and deformation is provided with the help of hydrodynamic and ultrasonic principles. Hydrodynamic computation of true or natural viscosities shows that ocean shear viscosity (η_G), compression viscosity (η_K), and extensional viscosity (η_E) are interrelated. There are no experimental methods available for the *in situ* measurement of these viscosities. Sound absorption coefficients (α_{obs}) allow to know the ultrasonic shear (η_{UG}), compression (η_{UK}), and longitudinal (η_L) viscosities, which decrease with increasing frequency and increase with increasing temperature, the flow activation energies having nearly equivalent values; pressure (depth) increase/decrease them at low/high frequencies. The viscosities η^*_{UG}, η^*_{UK}, η^*_L are approached at about 1000 KHz. They decrease with temperature and pressure, and increase with salinity. The η^*_{UG} becomes equal to the true shear viscosity η_G at the viscosity ratio $\delta = \eta_{UK} / \eta_{UG} = 0$.

Keywords: Chemical relaxation, ocean rheology, sound absorption, ultrasonic viscosity, viscosity ratio.

1. INTRODUCTION

The continuum mechanic approach to ocean flow and deformation (ocean rheology) has been described elsewhere [1]. It may be summarized as follows:

Turbulent diffusion prevails in the ocean over molecular diffusion. Molecular diffusion in simple fluids, as the ocean is assumed to be, is isotropic because it develops at those very small scales where stratification plays no role in inhibiting the vertical motions.

The molecular diffusion mechanism of actual seawater is provided by the physical structural relaxation of clusters [2] which contain associations with weak (water-water) and strong (ion-water) bonds with their corresponding relaxation times [3].

The molecular horizontal momentum transport of seawater is the result of three contributions: shear (η_G), extension (η_E), and compression (η_K)$^{(!)}$ flows [4] which are interrelated by Eq. (4) :

$$\eta_G = \frac{-\sigma_{12}}{\frac{\partial u}{\partial z}} = \frac{-\sigma_{12}}{\frac{1}{\Delta z}\frac{\Delta x}{\Delta t}} = \frac{-\sigma_{12}}{\dot{\gamma}_{12}} \quad (1)$$

$$\eta_E = \frac{-(\sigma_{11}-\sigma_{22})}{\frac{1}{L}\frac{\Delta L}{\Delta t}} = \frac{-(\sigma_{11}-\sigma_{22})}{\dot{\varepsilon}} = \frac{-N_1}{\dot{\varepsilon}} \quad (2)$$

$$\eta_K = \frac{-\Delta p}{\frac{1}{\rho}\frac{\Delta \rho}{\Delta t}} = \frac{-\Delta p}{\frac{1}{V}\frac{\Delta V}{\Delta t}} = \frac{-\Delta p}{\dot{\chi}} \quad (3)$$

*Address correspondence to this author at the Facultad de Ciencias del Mar, Campus Universitario de Tafira,35017 Las Palmas de Gran Canaria, Spain; E-mail: jaleman@dqui.ulpgc.es

$$h\,\eta_E + i\,\eta_G = j\,\eta_K \quad (4)$$

(!) The term compression viscosity, internationally accepted [5], is used instead of the traditional bulk viscosity.

being σ_{12}, $(\sigma_{11}- \sigma_{22}) = N_1$, and ΔP, the shear, extensional, and compression stresses, respectively ; $\dot{\gamma}_{12}$, $\dot{\varepsilon}$, $\dot{\chi}$, are the shear, extensional, and compression deformation rates ; h, i, j dimensionless parameters.

The effect of the system variables on these viscosities is as follows [1]:

η_G (1.0 - 1.5 x 10^{-7} dbar.s) is independent of shear rate $\dot{\gamma}_{12}$ (Newton law, Eq. (1)), and η_K (2 - 4 x 10^{-7} dbar.s) decreases with compression rate $\dot{\chi}$ (s^{-1}).

Temperature (T) decreases η_G (Table **1**) [1] and increases η_K (Table **2**) [1]. The Arrhenius equation flow activation energies are positive and negative respectively: ΔE_G = 4 kcal/mol, and ΔE_K = - 1 kcal/mol.

Table 1. Ocean True Shear Viscosities

Z (m)	P dbar	T °C	η_G[a] 10^{-7} dbar.s
10	1	23.58	0.92
100	10	16.69	1.01
500	50	11.87	1.25
1000	100	7.03	1.41
1500	150	5.48	1.48
20100	200	4.03	1.54

[a] Station B.

Salinity (S) increases both η_G and η_K, but almost unnoticeably.

1874-8376/09 2009 Bentham Open

Decreasing pressures (P) (depth z) reduce both η_G (Table **1**) and η_K (Table **2**) making the clusters to move vertically from a compressed (spheroidal) to an elongated (ellipsoidal) state.

Table 2. Ocean True Compression Viscosities

Z (m)	η_K[a] *vs* z 10^{-7} dbar.s	η_K[b] *vs* T 10^{-7} dbar.s	T ºC
10	0.20	4.12	25
100	0.40	4.06	20
500	1.20	3.99	15
1000	2.10	3.90	10
1500	3.00	3.80	5
2000	4.20	------	---

[a]T = 15ºC, $\dot{\chi}$ = 4.5 x 10^9 s^{-1}, δ = 3.5.

[b]χ = 6.5 x 10^8 s^{-1}, z = 250 m, δ = 3.5.

There are no experimental techniques available to date to corroborate these results, but the needed suplementary experimental information may be obtained with *in situ* measurements of ocean sound absorption.

Recent developments of measurement techniques on molecular viscosity by ultrasound may be found in the literature [6-8]. Main studies on the ocean where devoted to oil slicks [9], red algae blooms [10] or the marine microlayer [11]. However to our knowledge there are no studies on the behavior of ultrasonic viscosity on the whole water column of the ocean. In section 3-a we formulate the expression of the ocean sound absorption coefficients, next in section 3-c we discuss the effect of temperature on the seawater viscosity ratio, we follow discussing the effects of pressure (depth), temperature and salinity on ultrasonic viscosities, finally we conclude summarizing the main findings.

2. EXPERIMENTAL PROCEDURES

Sound absorption coefficients (α_{abs}) were measured with the method of sofar shots detonated at different ocean locations by [12] and references there on.

Viscosity ratios (δ) were deduced [1] from standard seawater shear viscosities [13] and ocean compressibility data [14].

3. RESULTS AND DISCUSSION

3.1. Ocean Sound Absorption Coefficients

The sound absorption coefficient (α_i) for a single relaxation process obeys the equation [15]:

$$\alpha_i = \frac{\pi \kappa_i}{\kappa_0 \, c} \frac{f_i f^2}{f_i^2 + f^2} \tag{5}$$

where κ_o is the isothermal compressibility (β is the symbol commonly used for compressibility in ultrasonics), κ_i the chemical compressibility (Table **3**) [16], c the sound velocity, f the acoustic frequency, and f_i the relaxation frequency which according to [17] is about 1 KHz for boric acid ($B(OH)_3$) (in this frequency range the contribution of scattering of inhomogeneities in the index of refraction of the medium is a constant independent of frequency, and amounts to 10^{-6} dB/m [18], about 10 KHz for magnesium sulfate ($MgSO_4$), and about 1,000 KHz for water (H_20).

Ocean sound absortion coefficients ($\alpha_{abs,}$ dB/m) may be obtained from data of [12] (which are also used to asses the potential effects of suspended particles and gas bubbles) with the following equations [17]:

At salinity S = 35 [4] (A, B, C, f_1, f_2, being temperature, pressure, and salinity dependent parameters):

$$\alpha_{obs} = \frac{A f_1 f^2}{f_1^2 + f^2} + \frac{B f_2 f^2}{f_2^2 + f^2} + C f^2 \tag{6}$$

The first, second, and third terms of the right -hand side of Eq. (6) are related to the relaxation mechanisms of the $B(OH)_3$ (carbonate modify it [4]), $MgSO_4$, and H_20, respectively. See Table **3** [16] in which are also shown the partial molal volume change of the solutes in sewawater ($\overline{\Delta V^*}$), and the partial molal compressibility of the solutes:

Table 3. Chemical Relaxation Mechanisms

Reaction	$\overline{\Delta V^*}$ cm^3 mol^{-1}		$\overline{\Delta \kappa^*}$ cm^3 mol^{-1} bar^{-1}	
	25ºC	5ºC	25ºC	5ºC
Acid-base equilibrium (non-electrolites):				
Water $H_2O \rightarrow H^+ + OH^-$	18.0	19.5	3.15	4.73
Boric acid $B(OH)_3 + H_2 0 \rightarrow H^+ + B(OH)_4^-$	25.7	28.0	1.93	2.79
Carbonic acid $CO_2 + H_2O \rightarrow CO_3H_2$	22.6	24.7	1.90	3.51
$CO_3H^- \rightarrow H^-CO_3^{2-}$	------	------	-----	------
Ion-pair equilibrium:				
$MgSO_4(aq) \rightarrow Mg^{2+}(aq) + SO_4^{2-}(aq)$	7.2	-------	1.7	--------

$$\overline{\Delta\kappa^*} = \overline{-\Delta V^*} / \Delta P \quad (7)$$

At S = 35 - 37 and frequency f = 2 - 25 KHz [19]:

$$\alpha_{obs} = 8.6866\left(\frac{2.34\times10^{-6} S f_T f^2}{f_T^2 + f^2} + \frac{3.38\times10^{-6} f^2}{f_T}\right)\left(1 - 6.54\times10^{-4} P\right) \quad (6a)$$

with the frequencies f and $f_T = 21.9 \times 10^{6\ -\ 1520/(T+273)}$ in KHz, TºC, P in atmosphere, and the factor 8.6866 to convert nepers/m into dB/m.

Seawater α_{obs} (Fig. **1**) behaves differently at frequencies of the order of the H_20 relaxation one (500-1,000 KHz), and shows a change of slope at about 15ºC. The molecular structure of pure water is [20] (Fig. **1c**): hexagonal (ice crystals) below 0ºC, tetrahedral (pentamer) above 5ºC, chain like (trimer) at about 27ºC, more than 10% of the water molecules have changed their tetrahedral structure to the chain one above 30ºC.

The ocean sound absorption coefficient is related to the ultrasonic shear (η_{UG}) and compression (η_{UK}) viscosities by the equation [17]:

$$\alpha_{theor} = \frac{16\pi^2 f^2}{3\rho c^3}\left(\eta_{UG} + \frac{3}{4}\eta_{UK}\right) = \frac{16\pi^2 f^2}{3\rho c^3}\eta_{UG} + \frac{4\pi^2 f^2}{\rho c^3}\eta_{UK} \quad (8)$$

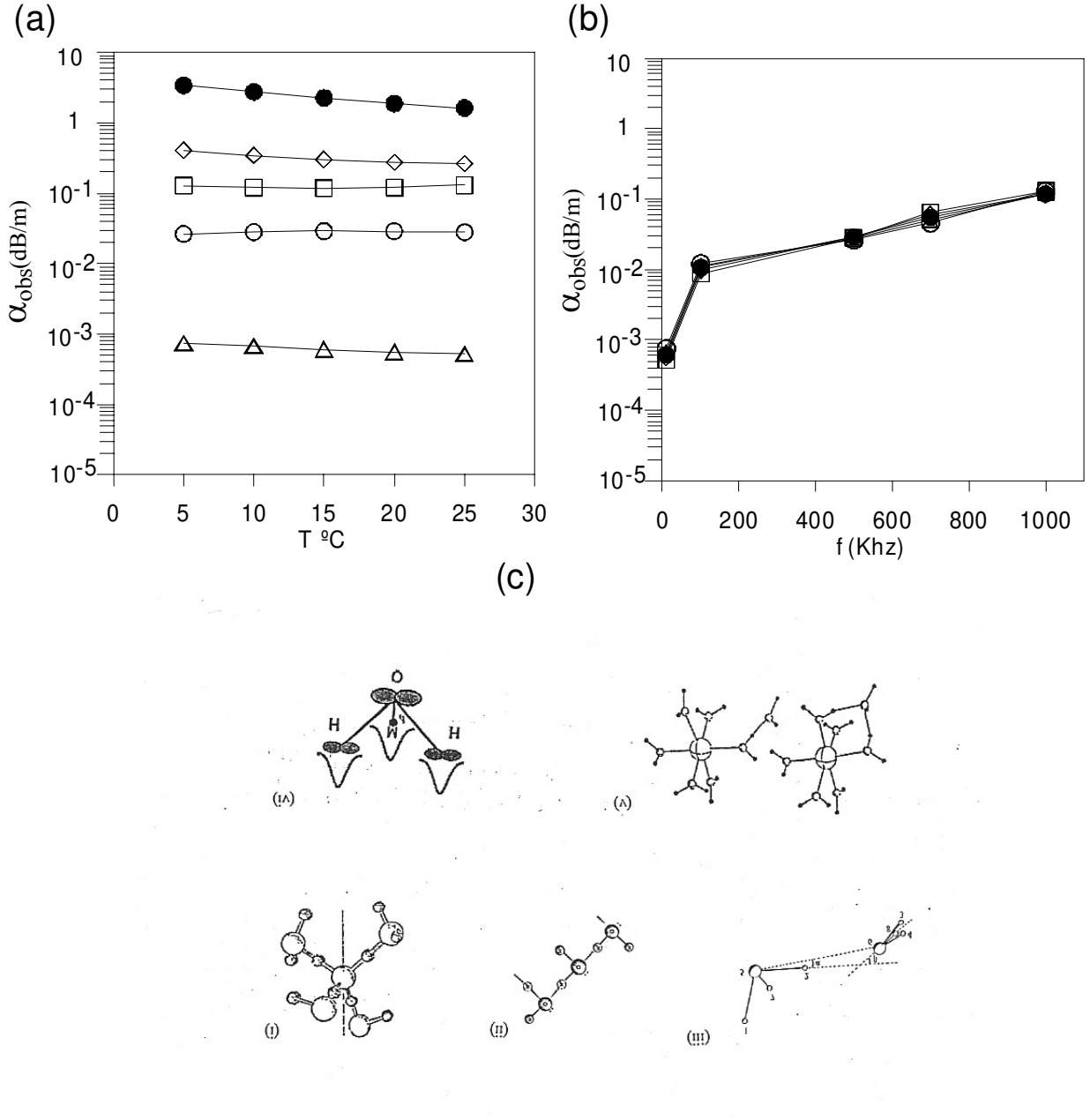

Fig. (1). Ocean sound absorption coefficient (α_{obs}) at S = 35, depth z = 1,000 m, δ = 3.2, (**a**) as a function of temperature at (Δ) 10 KHz, (○) 100 KHz, (□) 500 KHz, (◊) 1,000 KHz, (●) 3,000 KHz. (**b**) as a function of frequency at (○) 5ºC, (Δ) 10ºC, (●) 15ºC, (◊) 20ºC, (□) 25ºC. (**c**) Pure water structure: (**i**) pentamer ((●) hydrogen atom, (○) oxygen atom, from [24]), (**ii**) trimer (from [10].), (**iii**) dimer (from [25]), (**iv**) monomer (from [26]), (**v**) ion cluster illustrating one water molecule in the second layer (from [2]).

in which f is the frequency in Hz, and the viscosities expressed in poises, the density in g/cm^3, and the sound velocity c in cm/s calculated with the algorithm described by [17].

The first term of Eq. (8) is the absorption coefficient α_{class} in the low frequency limit, i.e., the shear viscous loss [4]:

$$\alpha_{class} = \frac{16\pi^2 f^2}{3\rho c^3}\eta_{UG} \tag{9}$$

3.2. Viscosity Ratio

The shear and compression viscosities are interrelated by the equation [1]:

$$\delta = \eta_{UK} / \eta_{UG} \tag{10}$$

Measurement of this dimensionless ratio provide $\delta = 2.81$ for seawater [18]. Seawater δ values at S = 35 - 37, T = 5ºC-25ºC, P = 1 - 2000 dbar, may be deduced as in [1].

Fig. (**2a**) is a typical example at S = 35 since: i) the η_G used are for standard seawater [13], ii) the effect of S on both η_G and η_K are almost unnoticeable [1], iii) Eq. (6) used to compute the sound absorption coefficients (α_{obs}) is valid only for S=35 [17]. As may be observed the plots are nearly straight lines and δ increases with increasing depth (z) and decreasing compression rate ($\dot{\chi}$).

The effect of temperature on the seawater viscosity ratio (Fig. **2b**) shows a different slope below and above 15ºC [1], what possibly is due to the fact that seawater is a dilute polymeric system consisting of 6-60 water molecules with an ion in the center (solvation shell) (Fig. **1c**). Under the pressure of sound waves the relaxation mechanism is a chemical association-dissociation reaction [15] giving rise to a large volume change upon ionization (Table **3**, [16]). Most seawater cations are in a 99% dissociated state, while magnesium sulfate ($MgSO_4$) is only 78.5% dissociated (Table **4**) [21]. As the temperature increases a decrease of both the partial molal volume change ($\overline{\Delta V^*}$) and the partial molal compressibility ($\overline{\Delta\kappa^*}$) occurs (Table **3**). The corresponding cluster structure expands decreasing the volume deformation ($\chi = (\Delta V / V)$) [1]. The final result is an increase in compression viscosity and viscosity ratio (Eqs. (3) and 10)).

The viscosity ratio δ of pure water has been measured [4] to be 2.68 -2.75 and is almost independent of depth (pressure), while it decreases slightly at all temperatures [4, 22] and, at frequencies of the order of GHz, decreases steeply below 15ºC (Figure 8 of [23]); compare with Fig. (**1a**) and Eq. (11).

3.3. Ultrasonic Viscosities

The ultrasonic compression viscosity (η_{UK}) is [4]:

$$\eta_{UK} = \frac{4}{3}\eta_{UG}\left(\frac{\alpha_{obs} - \alpha_{class}}{\alpha_{class}}\right) \tag{11}$$

Substituting in Eq.(11) the Eqs.(6-6a, 9, 10) results:

$$\eta_{UK} = \delta \cdot \eta_{UG} = \frac{4}{3}\eta_{UG}\left(\frac{\alpha_{obs}}{\alpha_{class}} - 1\right) \tag{12}$$

which allows to find the ultrasonic shear viscosity (η_{UG}) as follows (the factor 0.25 comes from 0.25 = (4/3) / (16/3)):

$$\delta \cdot \eta_{UG} = \frac{4}{3}\eta_{UG} \cdot \frac{\alpha_{obs}}{\frac{16\pi^2 f^2}{3\rho c^3}\eta_{UG}} - \frac{4}{3}\eta_{UG} = \frac{0.25 \cdot \alpha_{obs} \cdot \rho c^3}{\pi^2 f^2} - \frac{4}{3}\eta_{UG} \tag{13}$$

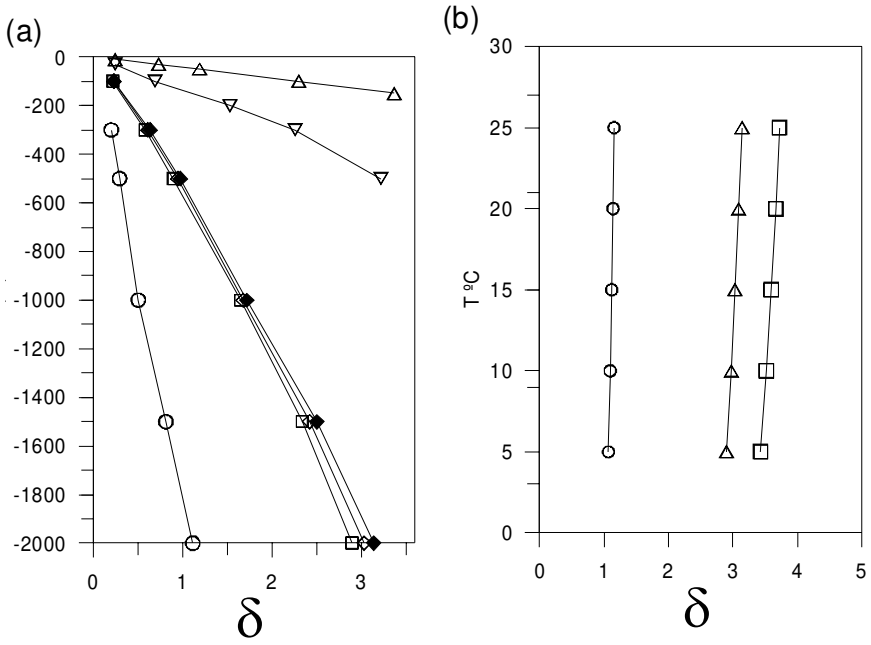

Fig. (2). Seawater viscosity ratio (δ) (**a**) at T = 15ºC, S = 35, as a function of depth (z) and different compression rates ($\dot{\chi}$): (Δ) 4.2 x 10^8 s^{-1}, (∇) 1.2 10^9 s^{-1}, ($\Diamond$) 4.25 x 10^9 s^{-1}, ($\blacklozenge$ = 25ºC, $\square$ = 5ºC), ($\circ$) 1.1 x 10^{10} s^{-1}. (**b**) as a function of temperature at S=35, z = 2,000 m, (Δ) $\dot{\chi}$ = 4.2 x 10^9 s^{-1}, ($\circ$) $\dot{\chi}$ = 1.1 x 10^{10} s^{-1}, ($\square$) 1.16 x 10^9 s^{-1} (z = 500 m).

Table 4. Dissociation States of Seawater Salts

Free Ions		% Associated With						
Cation	**g/kg (15)**	**%**					**SO_4^{2+}**	**CO_3H^-**
Sodium	10.733	99					1.2	0.01
Magnesium	1.294	87					11.0	1.0
Calcium	0.412	91					8.0	1.0
Potasium	0.339	99						
Strontium	0.0079							
Anion			Na^+	Mg^{2+}	Ca^{2+}	K^+		
Chloride	19.354	---------- reference ion----------						
Sulfate	2.712	54	21	21.5	2	0.5		
Bicarbonate	0.142	69	8	19.0	4	-----		
Carbonate	--------	9	17	67.0	4			
Borate	0.0045	0.01						
Bromide	0.067							
Fluoride	0.0013							

Therefore

$$\delta \cdot \eta_{UG} + \frac{4}{3}\eta_{UG} = \left(\delta + \frac{4}{3}\right)\eta_{UG} = \frac{0.25 \cdot \alpha_{obs} \cdot \rho\, c^3}{\pi^2 f^2} \qquad (14)$$

and (using the factor 10^{-2} to have the results with units 10^{-7} dbar.s) the ultrasonic shear viscosity is:

$$\eta_{UG} = \frac{0.25 \cdot 10^{-2} \cdot \alpha_{obs} \cdot \rho\, c^3}{\pi^2 f^2} \cdot \frac{1}{\delta + \frac{4}{3}} \qquad (15)$$

which at $\delta = 0$ is equivalent to Eq. (9) (see also Fig. **3d**).

The ultrasonic compression viscosity (η_{UK}) is obtained then from Eq. (12):

$$\eta_{UK} = \delta \cdot \eta_{UG} = \frac{0.25 \cdot 10^{-2} \cdot \alpha_{obs} \cdot \rho\, c^3}{\pi^2 f^2} \cdot \frac{\delta}{\delta + \frac{4}{3}} \qquad (16)$$

which at $\delta = 0$ becomes $\eta_{UK} = 0$ (Fig. **3f**).

The longitudinal viscosity (η_L) may be estimated as [18]:

$$\eta_L = \frac{4}{3}\eta_{UG} + \eta_{UK} \qquad (17)$$

Fig. (**3a**, **c**, **e**, **g**), show that the three viscosities η_{UG}, η_{UK}, η_L decrease with increasing frequency, becoming independent of it at about 20 KHz (Fig. **3b**). The viscosities η^*_{UG}, η^*_{UK}, η^*_L, shown in Fig. (**3d**, **f**, **h**), are approached at the H_20 relaxation frequency (1,000 KHz), as shown in Fig. (**3c**, **e**, **g**).

As δ decreases:

η^*_{UG} increases towards the true viscosity η_G (Table **1**) [1].

η^*_{UK} decreases towards $\eta^*_{UK} = 0$. It also decreases with temperature: note that this is contrary to what happens with continuum mechanics η_K values (Eq. 3) which increase with temperature (Table **2**) [1]. It is due to fact that the effect of temperature is different on the chemical asociation-dissociation relaxation than on the physical cluster structure relaxation. The activationn energies (ΔE) computed with Arrhenius equation [1] have nearly equivalent values (shear $\Delta E_{UG} = 2.46$ kcal/mol, compression $\Delta E_{UK} = 1.80$ kcal/mol, longitudinal $\Delta E_L = 2.10$ kcal/mol).

η^*_L is almost constant suggesting that (Eqs. (17) and (4)):

$$\eta_L^{*(\delta\to 0)} = \frac{4}{3}\eta_{UG}^{*(\delta\to 0)} + \eta_{UK}^{*(\delta\to 0)} \approx h\ \eta_E = -i\,\eta_G + j\,\eta_K \qquad (18)$$

It shows the effect on η_E of the strength of the cluster hydrogen bonds (which are, for example, stronger for Na^+ and weaker for Cl^-), and that the clusters are more compacted at large depths.

Fig. (**4a**) shows that as the temperature increases η_{UG}, η_{UK}, η_L increase at low frequencies up to 15ºC and decrease at higher temperatures for all frequencies. It is the result of the combined effects of the sound velocity c (increase with increasing temperature [17]), the sound absorption coefficient α_{obs} (Fig. **1**), and the viscosity ratio δ (Fig. **2b**). η^*_{UG}, η^*_{UK}, η^*_L (Fig. **4b**) decreases with temperature.

The effect of pressure (depth) is to increase η_{UG}, η_{UK}, and η_L (Fig. **4c**). The viscosities η^*_{UG}, η^*_{UK}, and η^*_L above 1,000 KHz (Fig. **4d**) decrease since increasing depth (P) decrease $\overline{\Delta\kappa^*}$ (equation 7).

The effect of salinity (S) on the ultrasonic viscosities can be known replacing Eq. (6) by Eq. (6a) in Eq. (15). Fig. (**4e**, **f**) show that the salinity increases the three viscosities since increasing salinity decreases $\overline{\Delta V^*}$ and $\overline{\Delta\kappa^*}$.

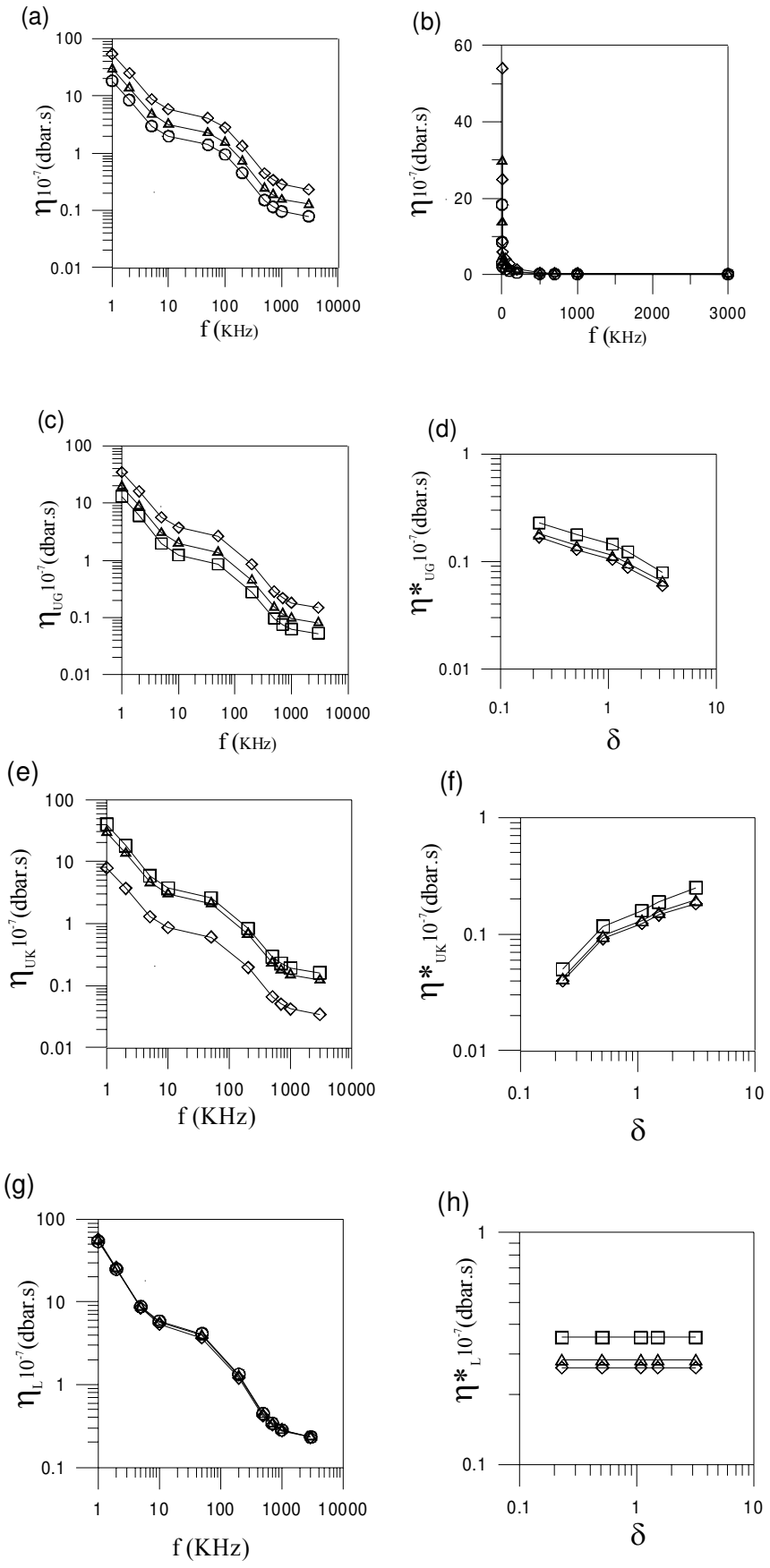

Fig. (3). Ultrasonic viscosities at T = 15ºC, S = 35, δ =1.52, as a function of frequency: (**a**) ((**b**) decimal plot) (○) η_{UG}, (Δ) $\eta_{UK,}$ (◊) $\eta_{L,}$ and at different viscosity ratios δ ((o) 80.23, (Δ) 1.52, (◊) 3.03, (**c**) $\eta_{UG,}$ (**e**) η^*_{UK}, (**g**) $\eta^*_{L.}$ As a function of δ at frequency f_i = 1,000 KHz and different temperatures (□) 5ºC, (Δ) 15ºC, (◊) 25ºC); (**d**) η^*_{UG}, (**f**) η^*_{UK}, (**h**) η^*_{L}.

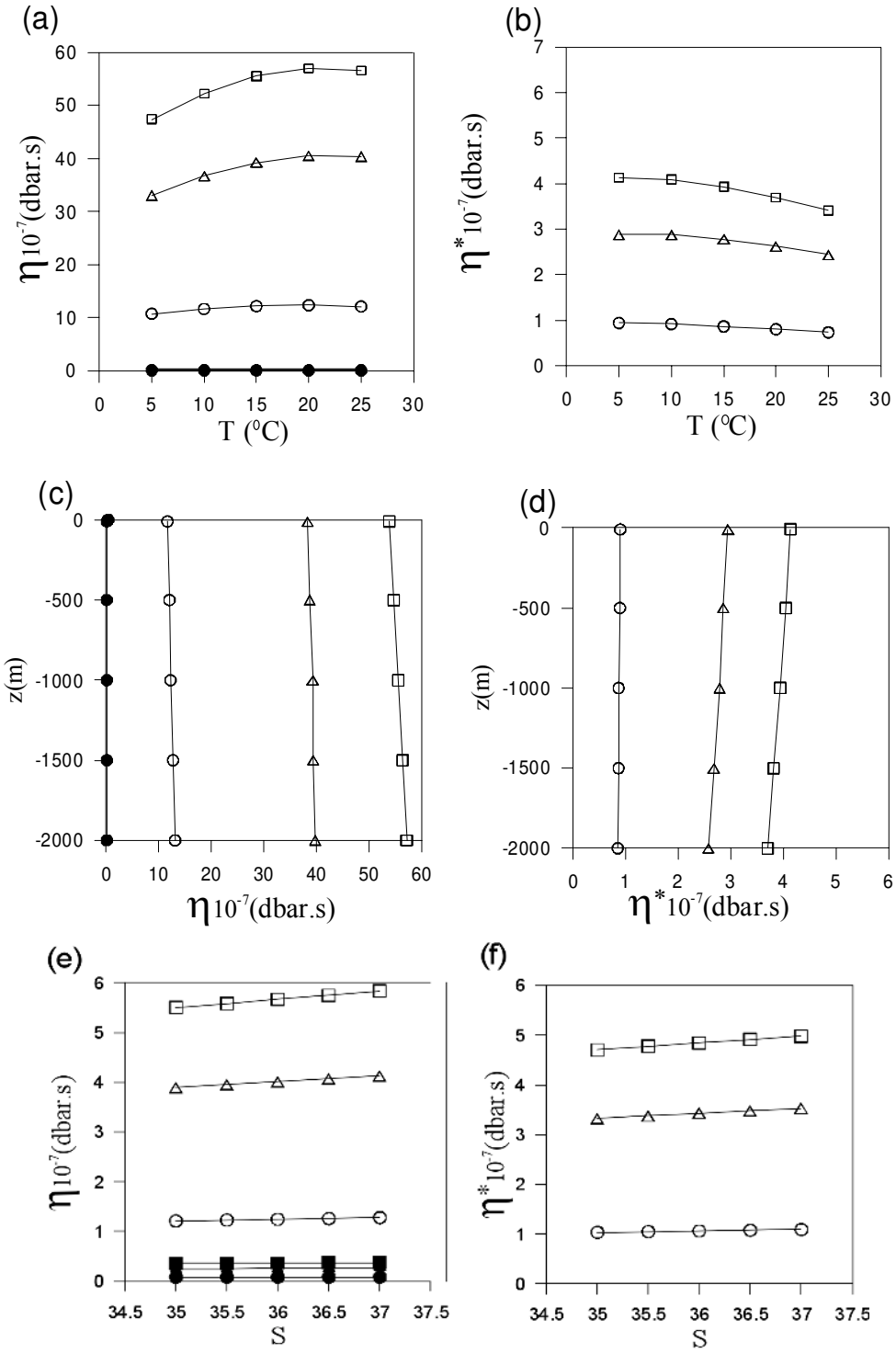

Fig. (4). Effect of temperature at S = 35, z = 1,000 m, δ = 3.2, on (**a**) (○) η_{UG}, (Δ) η_{UK}, (□) η_{L}, at frequency (white symbols) 1KHz, and (●) 700 KHz. (**b**) (○) η^{*}_{UG}, (Δ) η^{*}_{UK}, (□) η^{*}_{L} (f_i = 1,000 KHz). Effect of depth (z) at T = 15ºC, S = 35, δ = 3.2, and frequency (white symbols) 1 KHz, and (●) 700 KHz: on (**c**) (○) η_{UG}, (Δ) η_{UK}, (□) η_{L} ((●), □, at 700 KHz); (**d**) (○) η^{*}_{UG}, (Δ) η^{*}_{UK}, (□) η_{L} (f_i = 1,000 KHZ). Effect of salinity (S) at T = 15ºC, z = 1,000 m, δ = 3.21, and f = 10 KHz: (**e**) (○) η_{UG}, (◊) η_{UK}, (□) η_{L} ((●), ▼, ■, at 700 KHz) ; (**f**) at f_i = 1,000 KHz (○) η^{*}_{UG}, (Δ) η^{*}_{UK}, (□) η^{*}_{L}.

4. CONCLUSIONS

Seawater is a system which contains compressed hydrogen-bonded reversible ion networks (clusters) suspended in water oligomers. The molecular behavior of this system may be interpreted with two different approaches. The continuum mechanics with which the shear, extensional, and compression viscosities may be evaluated [1]. Ultrasonic measurements which show that ultrasonic shear, ultrasonic compression, and longitudinal viscosities decrease with frequency, increase/decrease with temperature,

and the pressure (depth) increase/decrease them at low and high frequencies, respectively. At the lower viscosity ratio (δ) the ultrasonic shear viscosity is similar to the continuum mechanics one.

ACKNOWLEDGMENTS

We thanks to J.L. Pelegri, co-author of the Ocean rheology (2006) article, for useful discussions. Partial support for this work has been provided by the Spanish government through project COUPLING (CTM2008-06343C02-01/ANT).

REFERENCES

[1] Aleman JV, Pelegrí JL, Sangrà P. Ocean rheology. J Non-Newtonian Fluid Mech 2006; 133: 121-31.

[2] Stace A. Cluster solutions. Science 2001; 294: 1292-3.

[3] Wang XB, Yang X, Nicholas JB, Wang LS. Bulk-like features in the photoemission spectra of hydrated double charged anion clusters. Science 2001; 294: 1322-5.

[4] Litovitz TA, Davis CM. In: Mason WP, Ed. Structural and shear relaxation in liquids, in physical acoustics. New York: Academic Press 1965; vol. IIA.

[5] Kaye A, Stepto RF, Work WJ, Aleman JV, Malkin AY. Definitions of terms relating to the non-ultimate properties of polymers. Pure Appl Chem 1998; 70: 701-54.

[6] Wygant IO, Kupnik M, Windsor JC, *et al.* 50 kHz Capacitive micromachined ultrasonic transducers for generation of highly directional sound with parametric arrays. IEEE Trans Ultrason Ferroelectr Freq Control 2009; 56(1): 193-203.

[7] Stephens DN, Cannata J, Liu R, *et al.* Multifunctional catheters combining intracardiac ultrasound imaging and electrophysiology sensing. IEEE Trans Ultrason Ferroelectr Freq Control 2008; 55(7): 1570-81.

[8] Huang Y, Zhang X, Haeggstrom EO, Ergun AS, Cheng C-H, Khuri-Yakub BT. Capacitive micromachined ultrasonic transducers (CMUTs) with isolocation posts. Ultrasonics 2008; 48: 74-81.

[9] Scott JC. Ocean surface slicks-pollution, productivity, climate andlife-saving. Geoscience and Remote Sensing Symposium, 1999. IGARSS '99 Proceedings. IEEE 1999 International 1999; vol 3: pp. 1463-8.

[10] Zhou C, Ma H. Ultrasonic degradation of polysaccharide from a red algae (*Porphyra yezoensis*). J Agric Food Chem 2006; 54 (6): 2223-8.

[11] Cinbis C, Despaux G, Robert L, Chou C-H, Khuri-Yakub BT. Ultrasonic in-situ measurement of the marine microlayer. Ultrason Symp Proc IEEE 1990; 2: 1057-60.

[12] Thorp WH. Deep ocean sound absorption in the sub- and low-kiilocycle-per-second region. J Acoust Soc Am 1965; 38: 648-54.

[13] Stanley EM, Batten RC. Viscosity of seawater at moderate temperatures and pressures. J Geophys Res 1969; 74: 3415-20.

[14] Sun S, Bleck R, Rooth C, Dikowicz J, Chassignet E, Killworth P. Inclusion of thermobaricity in isopicnic-coordinate ocean models. J Phys Oceanogr 1999; 29: 2719-29.

[15] Fisher FH, Simmons VP. Sound absorption in water. J Acoust Soc Am 1977; 62: 552-64.

[16] Millero FJ. In: Riley JP, Chester R, Eds. Chemical oceanography. USA: Academic Press 1983; vol. 8.

[17] Urick RJ. Principles of underwater sound. New York: McGraw-Hill 1975.

[18] Kinsler LE, Frey AL, Coppens AB, Sanders JV. Fundamentals of acoustics. New York: Wiley & Sons 1982.

[19] Schulkin M, Marsk HW. Sound absorption in water. J Acoust Soc Am 1962; 34: 864.

[20] Wernet Ph, Nordlun D, Berghman U, *et al*. The structure of the first coordination shell in liquid water. Science 2004; 304: 995-9.

[21] Garrels RM, Thompson ME. A chemical model of seawater at 25ºC and one atmosphere total pressure. Am J Sci 1962; 260: 57-66.

[22] Rouch J, Lai CC, Chen H. Brillouin scattering studies of normal and supercooled water. J Chem Phys 1976; 65: 4016-21.

[23] Xu J, Ren XR, Gong W, Dai R, Liu D. Measurement of the bulk viscosity of liquid by Brillouin scattering. Appl Opt 2003; 42: 6704-9.

[24] Whitfield M. In: Riley JP, Skirrow G, Eds. Chemical oceanography, 2nd ed. USA: Academic Press 1975; vol. 2.

[25] Niesar U, Corongiu G, Clementi E, Kneller GR, Braattacharya DK. Molecular dynamics simulation of liquid water using the NCC ab initio potential. J Phys Chem 1990; 94: 7949-56.

[26] Fanourgakis GS, Xantheas SS. The flexible, polarizable, Thole Type, interaction potential for water (TTM2-F) revisited. J Chem Phys 2006; 110: 4100-6.

Received: October 8, 2008 Revised: June 17, 2009 Accepted: July 6, 2009